

GaP/Si WIRE ARRAY SOLAR CELLS

Adele C. Tamboli*, Daniel B. Turner-Evans*, Manav Malhotra, Michael D. Kelzenberg, and Harry A. Atwater
Thomas J. Watson Laboratories of Applied Physics, California Institute of Technology, Pasadena, CA, U.S.A.

*These authors contributed equally to this work

ABSTRACT

Si wire arrays have recently demonstrated their potential as photovoltaic devices [1-3]. Using these arrays as a base, we consider a next generation, multijunction wire array architecture consisting of Si wire arrays with a conformal $\text{GaN}_x\text{P}_{1-x-y}\text{As}_y$ coating. Optical absorption and device physics simulations provide insight into the design of such devices. In particular, the simulations show that much of the solar spectrum can be absorbed as the angle of illumination is varied and that an appropriate choice of coating thickness and composition will lead to current matching conditions and hence provide a realistic path to high efficiencies. We have previously demonstrated high fidelity, high aspect ratio Si wire arrays grown by vapor-liquid-solid techniques, and we have now successfully grown conformal GaP coatings on these wires as a precursor to considering quaternary compound growth. Structural, optical, and electrical characterization of these GaP/Si wire array heterostructures, including x-ray diffraction, Hall measurements, and optical absorption of polymer-embedded wire arrays using an integrating sphere were performed. The GaP epilayers have high structural and electrical quality and the ability to absorb a significant amount of the solar spectrum, making them promising for future multijunction wire array solar cells.

INTRODUCTION

Silicon wire array solar cells have recently demonstrated up to 96% absorption despite less than 5% packing fraction [1], 2-3% efficiencies in liquid electrolyte [2], and up to 8% efficiencies in large-area wire array solar cells [3]. We consider here an extension of these results to design of a multijunction wire array architecture consisting of Si wire arrays with a conformal wide bandgap III-V absorber layer. For an optimized two-junction cell, the bottom cell should have a band gap of approximately 1.1 eV and the top cell should have a band gap of approximately 1.7 eV [4]. Silicon and $\text{GaN}_x\text{P}_{1-x-y}\text{As}_y$ are good candidate materials for a two-junction cell, as they can be grown lattice matched and with near-optimum band gaps, given the proper choice of N, P, and As composition [4]. Two-junction cells using these materials could potentially reach a theoretical maximum efficiency of 37% without concentration and 44% with 500x concentration [4]. The performance of GaNPAs solar cells synthesized to date has been limited by short minority carrier diffusion lengths, suggesting that $\text{GaN}_x\text{P}_{1-x-y}\text{As}_y/\text{Si}$ solar cells may benefit from radial pn junctions formed in a wire array geometry, where the directions of light absorption and carrier collection are orthogonalized. Wire arrays also provide effective concentration without the need for

external optics as they can absorb nearly all the incident light despite having a $2.8 \mu\text{m}$ planar equivalent volume [1]. GaP provides a model system for beginning to explore multijunction wire array solar cells because it is nearly lattice matched to Si, and, while its band gap of 2.26 eV is larger than would be optimal for a dual-junction solar cell, GaP layers reported to date exhibit better minority carrier transport properties than GaNPAs with well understood material properties. Here, we explore light absorption and carrier transport via device physics simulations and microscopy, as well as electrical, and optical characterization of epitaxial GaP on Si wire array structures.

SIMULATIONS

As the performance of a GaP/Si solar cell will be current limited by the GaP, the light absorption properties of the GaP layer must be understood and optimized. We began by considering the angular absorption of a two-dimensional GaP on Si "grating," using full field electromagnetic simulations. We considered a $1 \mu\text{m}$ thick, $20 \mu\text{m}$ tall Si core with GaP thicknesses that varied from 0.5 to $2 \mu\text{m}$ in $0.5 \mu\text{m}$ increments. The two-dimensional slabs were placed $7 \mu\text{m}$ apart (Fig. 1). Boundary conditions for the top, sides, and bottom were fully absorptive (PML), periodic, and fully reflecting, respectively. The reflecting layer mimics a back reflector. Optical constants were taken from ref. [5]. A plane wave source at a varying wavelength and incident angle was used for excitation. The power absorbed in the GaP was then calculated and normalized to the incident power. As seen in Fig. 1, the outer GaP layer absorbed up to 80% of the above-band gap incident power, with losses primarily due to absorption by the Si core and by reflection, especially at normal incidence where much of the light misses the GaP entirely, simply traveling in between the GaP structures and reflecting back out of the grating. The location of the direct band gap in GaP is evidenced by the rapid increase in absorption at shorter wavelengths.

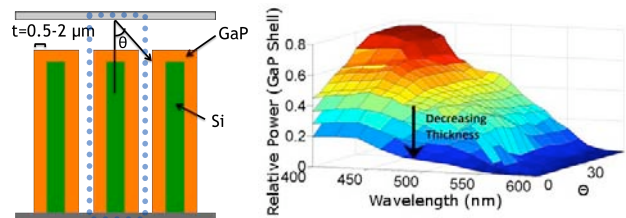


Figure 1. Simulated two-dimensional GaP/Si "grating" absorption. The simulation unit cell is outlined by the dotted box.

With our Si wire arrays, we have shown experimentally that we can minimize losses due to reflection and transmission through the array by incorporating antireflective coatings, scattering particles in between the wires, and a back reflector, resulting in peak absorption of 96%[1]. This suggests that with a thick GaP layer of about 2 μm along with appropriate light trapping techniques, we can absorb almost all the above-band gap incident light in the GaP layer.

We also considered a more realistic, full three-dimensional, periodic wire array, as shown in Fig. 2. This structure consisted of a 1 μm diameter, 10 μm tall Si wire with a 0.5 μm thick GaP shell, a 7 μm pitch, and the same boundary conditions used above. Computational limits forced us to reduce the length of the wire and the GaP thickness, and to only consider normal incidence. These conditions give us a lower bound for actual absorption, as typical wires can be up to 100 μm long, have GaP coatings of more than a micron, and have maximized absorption at oblique angles of incidence. As a point of comparison, we calculated the exponentially decaying Beer-Lambert absorption of the wire arrays as well. The results are shown in Fig. 2, where relative power refers to the amount of power absorbed in the listed material as normalized to the total incident power.

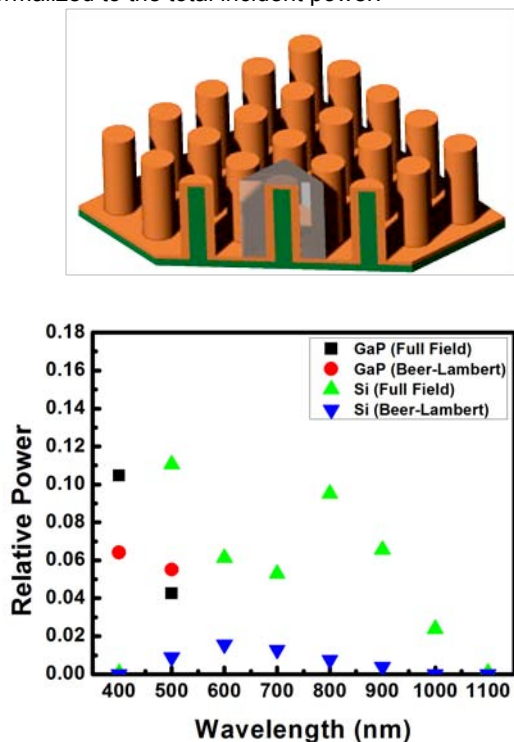


Figure 2. Normal incident GaP/Si wire array absorption. The simulation unit cell is outlined in the top diagram.

However, moving to 500 nm, the full field value falls significantly below the Beer-Lambert calculation. Looking first at the GaP absorption, we see that at 400 nm, where the GaP is fully absorbing, the full field absorption cross section is larger than would be expected from mere geometric, Beer-Lambert considerations. Examining the Si absorption, we see that this loss of power in the GaP corresponds to an increase in the Si absorption; the GaP refracts and focuses the incident beam, channeling light into the higher index Si core. Overall, Si absorption is greatly enhanced over much of the spectrum due to the GaP shell. Thus a relatively thick GaP layer is required to maximize shell absorption before light is lost to the Si core, or a direct band gap material should serve as the outer layer. Note that while the relative powers are low due to much of the light missing the structure entirely, we believe that we will be able to boost overall absorption by employing the light trapping techniques described in ref [1].

As GaNPs compounds have a smaller, direct band gap, we also explored the optical properties of GaAs for our shell. GaP and GaAs provide useful bounds for the behavior of GaNPs, as their band gaps lie on either side of GaNPs, and GaNPs can be either direct or indirect gap depending on the composition. As seen in Fig. 3, the shell absorption increases drastically, and once again, the absorption cross section is much greater than the geometric, analytical value. By weighing the simulated relative power absorption at 400 nm by the solar flux between 280 and 450 nm and the other powers by the solar flux in 100 nm bins on either side of the simulated wavelength, we calculated the current that would be expected in the shell and core for the two structures. The GaP/Si wire array generates 0.63 mA/cm² in the GaP shell and 2.60 mA/cm² in the Si core while the GaAs/Si wire array generates 4.20 mA/cm² in the shell and 0.22 mA/cm² in the core. Thus, the two structures fall on either side of current matching conditions and suggest that with an intermediate material and appropriate thickness choices the wire array cell can achieve current matching, and with light trapping techniques, high efficiencies.

For the GaP/Si wire arrays, we constructed full three-dimensional device physics models of the structure identical to those used in the three-dimensional optical simulations. We employed the device physics simulation tool Sentaurus, which calculates Poisson's equation and the carrier transport equations for a wide range of physical models and conditions. The model fidelity has been previously extensively validated using Si radial pn junction wire arrays in this format [6]. We began by considering GaP radial pn junction arrays on Si supports, considering top incident, Beer-Lambert absorption, varying the GaP thickness as in our two-dimensional model, and placing contacts on the outer GaP emitter and either on the Si or GaP base.

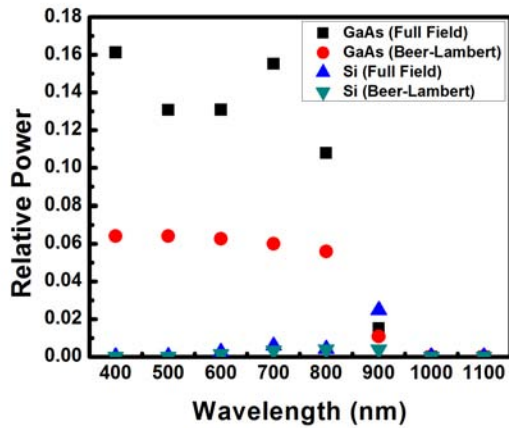


Figure 3. Normal incident GaAs/Si wire array absorption

The location of the base contact was found to have minimal influence on the properties of the cells as the conduction band offset between GaP and Si is small [7], and we considered a GaP cell with an n-type base with a doping of $1 \times 10^{17} \text{ cm}^{-3}$ and a p-type emitter with a doping of $5 \times 10^{18} \text{ cm}^{-3}$. Additionally, we varied the GaP diffusion length by modifying the lifetime in the material. The surface recombination velocity was assumed to be 0 for this simple model. As demonstrated in Fig. 4, optimal efficiencies were found for GaP thicknesses on the order of the material diffusion length, a result also seen in modeling of Si wires.

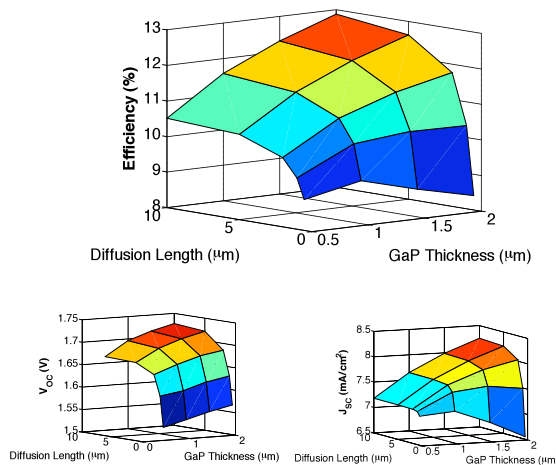


Figure 4. Simulated GaP/Si wire array efficiency, open circuit voltage (V_{oc}), and short circuit current (J_{sc}) contour plots assuming Beer-Lambert absorption

While the open circuit voltage falls off directly with diffusion length, having little dependence on thickness, the short circuit current reaches a maximum value when the diffusion length is comparable to the thickness, as would be expected for a radial junction geometry where generated carriers have to travel the shell thickness to be collected.

As seen in the aforementioned GaP/Si optical modeling, however, the Beer-Lambert model does not provide a realistic description of the optical absorption behavior of the arrays as the Si and GaP features are of comparable size to the excitation wavelength. Thus, optical generation profiles at a variety of wavelengths were obtained from the full field simulations, weighted appropriately by the solar spectrum, summed, and the whole inserted into the device physics simulation. Whereas in Fig. 4, the J_{sc} was calculated assuming that all incident light was absorbed in the wires, our more thorough model assumed that the whole wire array was illuminated, and hence much of the light failed to strike the wires and reflected out of the array without being absorbed. For a $10 \mu\text{m}$ diffusion length, the Beer-Lambert efficiency for $0.5 \mu\text{m}$ GaP thickness was calculated to be 0.97% while the full field value was found to be 0.80%, a decrease due to the GaP lensing effect. While we should be able to boost the J_{sc} through light trapping techniques, photons will still be directed from the shell into the higher index Si core, lowering the shell absorption.

These simulations suggest that a heterostructure wire array should be able to absorb much of the solar spectrum across a range of angles. Additionally, to attain current-matching conditions, the Si core thickness should be minimized while the shell thickness is maximized for indirect, large band gap compounds, whereas thinner wide band gap layers are need for current matching of direct, band gap compounds.

EXPERIMENTAL

We have previously developed a template-based vapor-liquid-solid (VLS) growth technique which produces high fidelity, high aspect ratio silicon microwire arrays using inexpensive chlorosilane precursors [8]. The wire arrays used here range in height from 10-50 microns and are 1-2 microns in diameter, as determined by the catalyst particle size during VLS growth and growth time. To coat these wire arrays in gallium phosphide, we use metalorganic chemical vapor deposition (MOCVD) using trimethyl gallium and phosphine precursors. Depending on the V/III ratio during growth, these layers are either p-type or n-type. In each growth, we included several pieces of planar silicon with the wire arrays to compare growth on planar and wire array substrates.

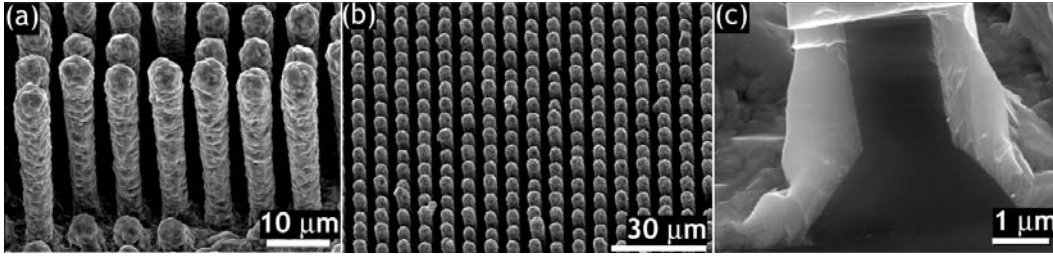


Figure 5. Scanning electron microscope images of GaP/Si wire arrays.

Figure 5 shows SEM images of GaP-coated Si wire arrays. A cleaved wire (Fig. 5(c)) shows the Si core and GaP coating in cross section. The GaP coating is conformal and rough, both on the wire array samples and the planar Si substrates, indicating that the roughness of the layer is caused by the polar on nonpolar nature of the epitaxy rather than the nature of the substrate [9]. X-ray diffraction measurements (Fig. 6) show that the layers are epitaxial, $\langle 111 \rangle$ oriented GaP films for both the wire array samples and planar samples, although there is a small $\langle 220 \rangle$ peak arising in all the wire array samples studied, which could be an artifact of the lower-quality nucleation layer grown first, visible only in the wire array samples because of their relatively thin epitaxial layer, or could be a product of misoriented wires that have broken off during handling of the samples.

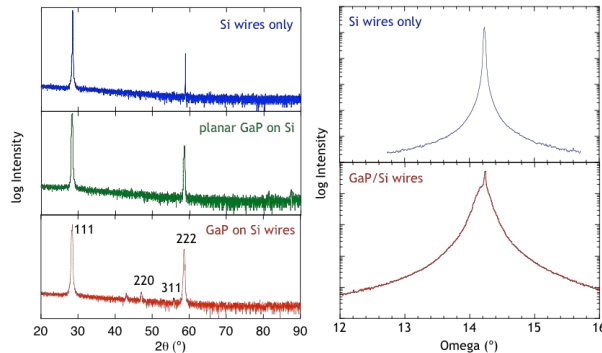


Figure 6. X-ray diffraction measurements of GaP/Si and Si samples. Top: ω - 2θ scans. Bottom: rocking curves.

Using epitaxially grown planar GaP on Si(111) substrates, we have performed Hall measurements at room temperature to determine resistivity, doping density, and mobility in GaP epilayers. Our n-type layers, which are grown using a V/III ratio of 80, have a carrier concentration of $8 \times 10^{16} \text{ cm}^{-3}$ and a mobility of $300 \text{ cm}^2/\text{Vs}$. Our p-type samples, which are grown using a V/III ratio of 10, have a carrier concentration of $1 \times 10^{18} \text{ cm}^{-3}$ and a mobility of $8 \text{ cm}^2/\text{Vs}$. Doping was achieved solely by changing the V/III ratio during growth; no additional impurities were added. GaP pn diodes were fabricated on our planar samples as well, with electrical contacts placed on the n- and p-type GaP. These diodes exhibited rectifying behavior with low leakage current. Under 1 sun illumination, these diodes

have an open circuit voltage of 660 mV, a short circuit current of 0.17 mA/cm^2 , and a fill factor of 42%. More details regarding structural and electrical characterization of our GaP layers are given elsewhere[10].

To understand light absorption in GaP/Si wire arrays, optical absorption studies were performed using an integrating sphere and wire arrays which have been embedded in a transparent polymer and peeled off the substrate[1]. Two wire arrays were studied: a Si wire array with $1.5 \mu\text{m}$ diameter, $30 \mu\text{m}$ long wires in a square array, and a GaP-coated array grown on a Si wire array substrate with the same properties as the bare Si wire array.

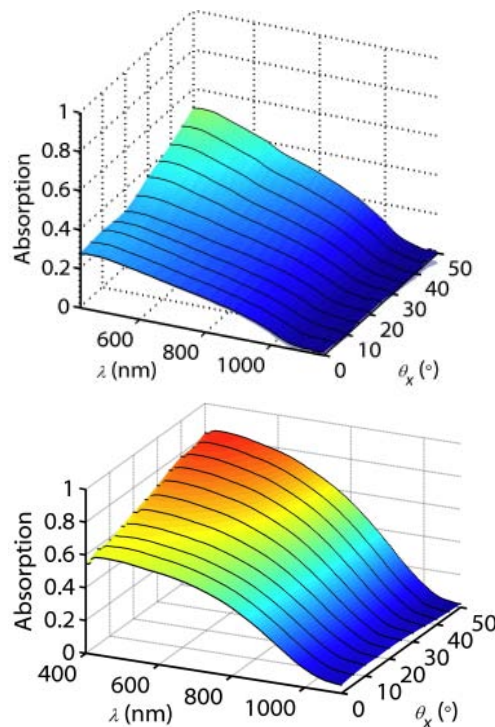


Figure 7. Optical absorption of peeled-off wire arrays: Top: Si wires only, Bottom: GaP-coated Si wires.

To find optical absorption, we measure reflection and transmission through GaP/Si wire arrays as a function of angle of incidence and wavelength. Figure 7 shows optical absorption in both Si and GaP/Si wire arrays. The

optical absorption is significantly enhanced by the addition of the GaP coating, and we are able to achieve nearly 100% absorption in our GaP/Si wire arrays without any explicit light trapping structure. The absorption enhancement is most likely caused by two factors: the higher fill factor of the GaP coated wires and scattering caused by the rough GaP surface, evidenced by the enhanced absorption even below the band gap of GaP. Additionally, the optical modeling reveals the wires exhibit a large absorption cross section and the GaP layer focuses light into the Si core, providing additional pathways for absorption enhancement over simply geometric considerations.

CONCLUSIONS

We propose Si/GaNPs wire array solar cells based on a conformal coating of GaNPs on VLS-grown Si wire arrays. Electromagnetic and device physics simulations guide our design of these structures, suggesting that much of the solar spectrum can be absorbed across angles of incidence and that appropriate thickness and band gap choice can lead to an efficient cell. We have been able to experimentally realize initial GaP/Si wire structures via MOCVD growth. The GaP/Si layers are conformal and epitaxial, and we have observed enhanced absorption compared to bare Si wire array structures.

ACKNOWLEDGEMENTS

The authors would like to acknowledge Greg Kimball and Emily Warmann for help with material characterization. This work was supported by the Defense Sciences Office of the Defense Advanced Research Projects Agency (DARPA). D.T.E. acknowledges support from the National Science Foundation in the form of a graduate research fellowship.

REFERENCES

- [1] M.D. Kelzenberg et al., "Enhanced absorption and carrier collection in Si wire arrays for photovoltaic applications", *Nature Mat.* **9**, 2010, pp. 239-244.
- [2] S.W. Boettcher et al., "Energy-Conversion Properties of Vapor-Liquid-Solid Grown Silicon Wire-Array Photocathodes", *Science* **327**, 2010, pp. 185-187.
- [3] M.C. Putnam et al., "Si Microwire Array Solar Cells", *Energy Environ. Sci.*, in press.
- [4] J.F. Geisz and D.J. Friedman, "III-N-V semiconductors for solar photovoltaic applications", *Semicond. Sci. Tech.* **17**, 2002, pp. 769-777.
- [5] D.E. Aspnes and A.A. Studna, "Dielectric functions and optical parameters of Si, Ge, GaP, GaAs, GaSb, InP, InAs, and InSb from 1.5 to 6.0 eV", *Phys. Rev. B* **27**, 1983, pp. 985-1009.
- [6] M.D. Kelzenberg, M.C. Putnam, D.B. Turner-Evans, N.S. Lewis, and H.A. Atwater, "Predicted efficiency of Si wire array solar cells", *34th IEEE PVSC*, 2009, pp. 1948-1953.
- [7] I. Sakata, M. Yamanaka, et al. "Characterization of heterojunctions in crystalline-silicon-based solar cells by internal photoemission." *Solar Energy Materials and Solar Cells* **93** (6-7), 2009, pp. 737-741.
- [8] B.M. Kayes et al., "Growth of vertically aligned Si wire arrays over large areas ($>1 \text{ cm}^2$) with Au and Cu catalysts", *Appl. Phys. Lett.* **91**, 2007, pp. 103110.
- [9] V.K. Dixit et al., "Effect of two-step growth process on structural, optical and electrical properties of MOVPE-grown GaP/Si", *J. Cryst. Growth* **310**, 2008, pp. 3428-3435.
- [10] A.C. Tamboli, M. Malhotra, G.M. Kimball, D.B. Turner-Evans, and H.A. Atwater, "Conformal GaP layers on Si wire arrays for solar energy applications", submitted, June 2010.